Cemented Carbides: Metallographic Techniques and Microstructures
Martin N. Haller, Staff Engineer, Kennametal, Inc.

<Previous section in this article

Atlas of Microstructures for Cemented Carbides

Fig. 1 Free (excess) carbon appears as clustered dark spots on this fracture surface of a cemented carbide. As-polished. 21×

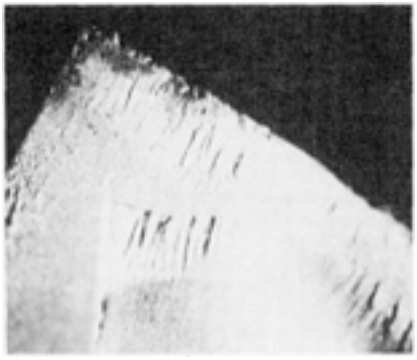

Fig. 2

Fig. 3

Carbon deficiency (η phase) on a fracture surface of cemented carbide. Fig. 2: before etching, η phase appears as shiny stringers, dots, and clusters. Fig. 3: after etching 5 s in Murakami's reagent, η phase is black.

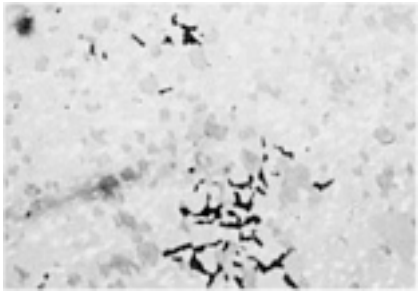

Fig. 4 86WC-8(Ta,Ti,Nb,W)C-6Co alloy, 91.6 HRA. An example of C-porosity (see Ref 5). Black areas are porosity, some of which still contain graphite (dark gray) distributed at grain boundaries of tungsten carbide particles (light gray, angular) and mixed carbides (darker gray, irregular, and rounded). Cobalt binder is white. As-polished. 1500×

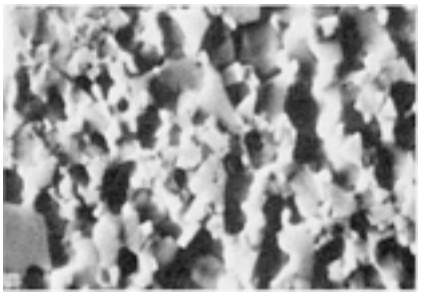

Fig. 5 Scanning electron micrograph of 79WC-14(Ta,Ti,Nb,W)C-7Co alloy, 92.2 HRA. Raised areas are cobalt binder; gray particles in intermediate areas are tungsten carbide; rounded, deeply etched particles are mixed carbides. Murakami's reagent (see Table 2), 2 min. 3000×

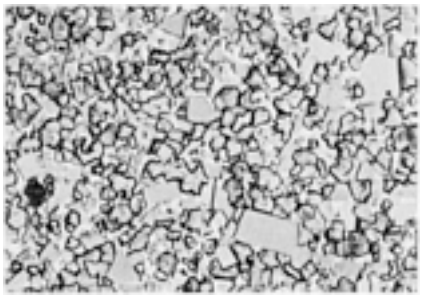

Fig. 6 80WC-13(Ta,Ti,Nb,W)C-7Co alloy, 92.2 HRA. White matrix is cobalt binder; light gray, angular areas are tungsten carbide; darker gray, rounded particles are mixed carbides. Murakami's reagent, 2 min. 1500×

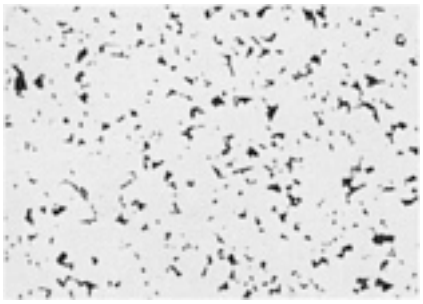

Fig. 7 Same specimen as Fig. 6, except etched to remove only the cobalt binder phase. Black areas are the removed binder phase. The photographic printing technique used suppresses the unetched tungsten carbide and mixed carbide particles. $FeCl_3$ (see Table 2), 10 s. 1500×

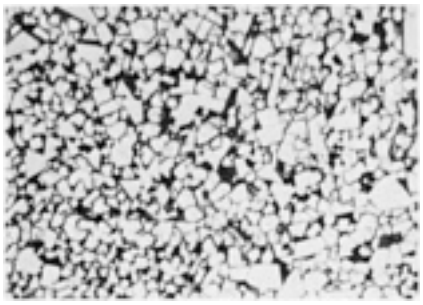

Fig. 8 Same specimen as Fig. 6. Binder and grain boundaries are black; angular, light gray particles are tungsten carbide; rounded, gray particles are mixed carbides. Murakami's reagent, 2 min, followed by $FeCl_3$, 10 s. 1500×

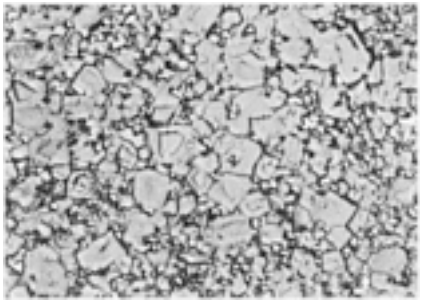

Fig. 9 5WC-8Mo-79TiC-8Ni alloy, 93.8 HRA. Irregular, gray shapes are complex carbides, many of which have a central core of unreacted titanium carbide. The fine, dark particles are overetched tungsten carbide and complex carbides; the nickel binder is white. Hot H_2O_2, 4 min (see Table 2). 1500×

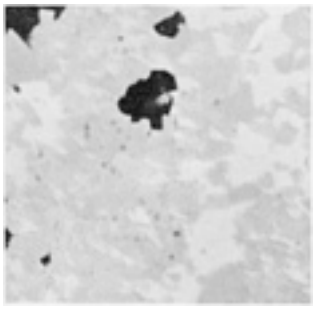

Fig. 10

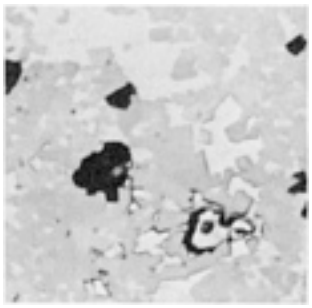

Fig. 11

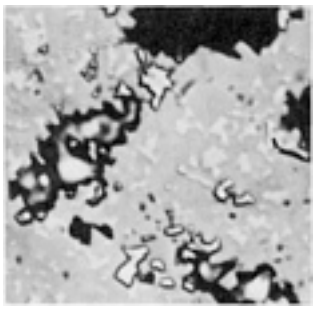

Fig. 12

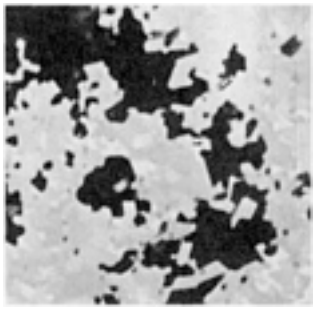

Fig. 13

89WC-10(Ta,W)C-1Co alloy, 94 HRA. Four micrographs of the same field showing progressive etching of W_2C. Fig. 10: black areas are porosity, and white phase is W_2C. Fig. 11: some W_2C (white) is deeply etched, and some is unetched, depending on orientation of the grains. Fig. 12: deeply etched W_2C (white); black areas are porosity or completely removed W_2C. Fig. 13: white areas are unetched W_2C or cobalt binder; black areas are completely removed W_2C or porosity. Gray, angular WC particles remain unetched throughout. Fig. 10: as-polished. Fig. 11: dilute ($\frac{1}{10}$ strength) Murakami's reagent, 10 s. Fig. 12: dilute Murakami's reagent, 30 s. Fig. 13: full-strength Murakami's reagent, 30 s. 2000×

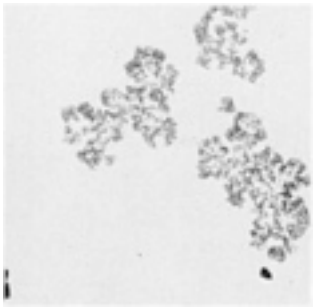

Fig. 14 85WC-8(Ta,Ti,Nb,W)C-7Co alloy, 90.3 HRA. Typical dendritic structure of η phase ($(Co_3W_3)C$). The composition of the phase was confirmed using x-ray diffraction techniques. Murakami's reagent, 3 s. 100×

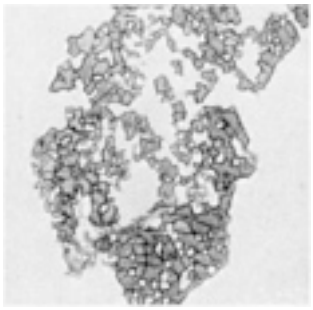

Fig. 15 Same alloy and etch as Fig. 14. Micrograph shows preserved $(Co_3W_3)C$ (M_6C) on an

undifferentiated cemented carbide background. The $(Co_3W_3)C$ phase is highly colored under bright-field illumination. 500×

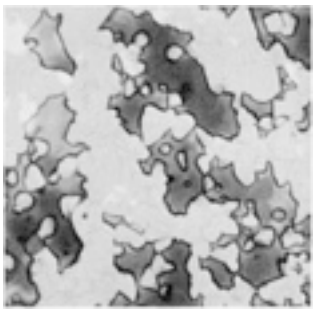

Fig. 16 Same alloy and etch as Fig. 14. $(Co_3W_3)C$ phase is dark gray with black etch boundaries. The varying shades of gray are due to the different colors of the phase. Background consists of angular, gray tungsten carbide particles, rounded, gray mixed carbides, and white cobalt binder. 1500×

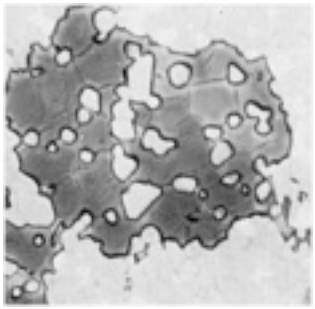

Fig. 17 Same alloy and etch as Fig. 14. Micrograph shows $(Co_3W_3)C$ η phase detail. Eta phase is various shades of gray with clear grain boundaries; light gray tungsten carbide particles surrounded by η phase are rounded due to solubility of the binder. 1500×

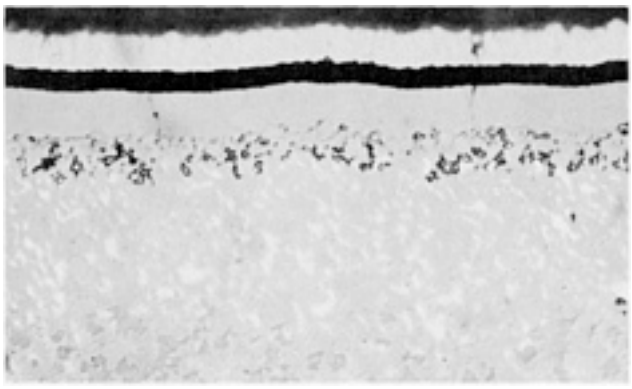

Fig. 18 85WC-9(Ta,Ti,Nb,W)C-6Co alloy substrate (92 HRA), coated for high speeds and feeds in cutting low-carbon steels. Microstructure shows (from bottom) cemented carbide substrate, $(Co_6W_6)C$ $(M_{12}C)$ η phase at interface of coating and substrate, TiC coating, Al_2O_3 coating, and TiN coating. $M_{12}C$ phase is the result of a decarburizing reaction during chemical vapor deposition of the refractory films. Murakami's reagent, 3 s. 1335×

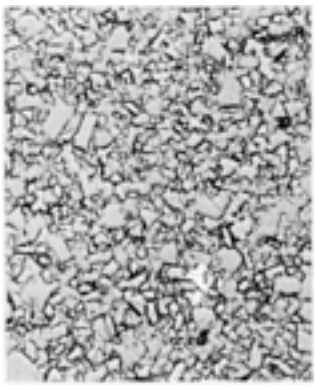

Fig. 19 97WC-3Co alloy, 93.2 HRA. Gray particles are WC, dark, overetched spots are mixed carbides; white particles are cobalt binder. Using ASTM standard B 390, this microstructure would be classified type 3-F (3, cobalt content; F, fine-grained structure). Murakami's reagent, 2 min. 1500×

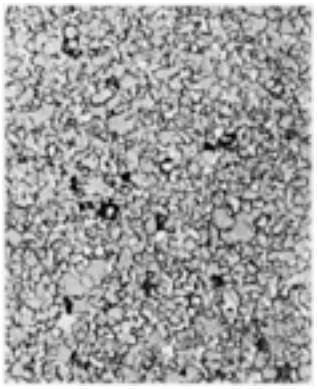

Fig. 20 92WC-2(Ta,W)C-6Co alloy, 92.7 HRA. Gray particles are tungsten carbide, and white areas are cobalt binder. The increased cobalt content is apparent when this figure is compared with Fig. 19. Murakami's reagent, 2 min. 1500×

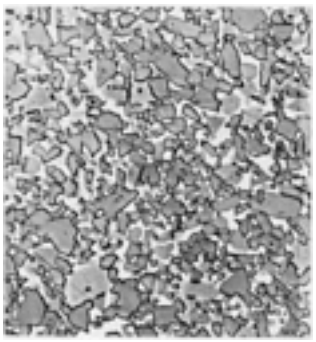

Fig. 21 89WC-11Co alloy, 89.8 HRA. Gray particles are tungsten carbide; white particles are cobalt binder in this medium-size grain structure. Note how HRA decreases as cobalt concentration increases (compare with Fig. 19 and 20). Murakami's reagent, 2 min. 1500×

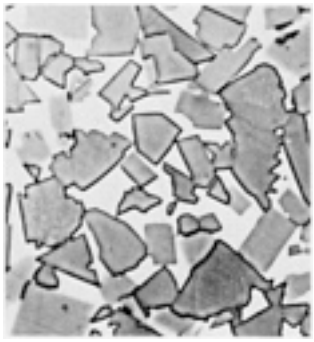

Fig. 22 85WC-15Co alloy, 84.9 HRA. This is a coarse structure, with tungsten carbide particles (gray, faceted particles in the white cobalt binder phase). Again, HRA has decreased as cobalt content has increased. Murakami's reagent, 2 min. 1500×

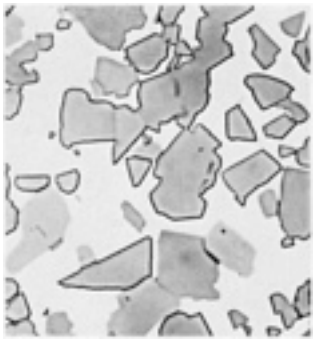

Fig. 23 75WC-25Co alloy, 79.3 HRA. Another coarse structure, with gray tungsten carbide particles in the white cobalt matrix. Compare HRA and cobalt content with the previous four figures. Murakami's reagent, 2 min. 1500×

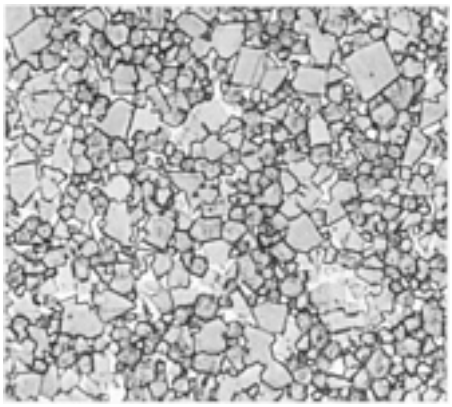

Fig. 24 83WC-10(Ta,Ti,Nb,W)C-8Co alloy, 90.3 HRA. Angular, gray particles are tungsten carbide; rounded, dark particles are mixed carbides; white particles are cobalt binder. Murakami's reagent, 2 min. 1500×

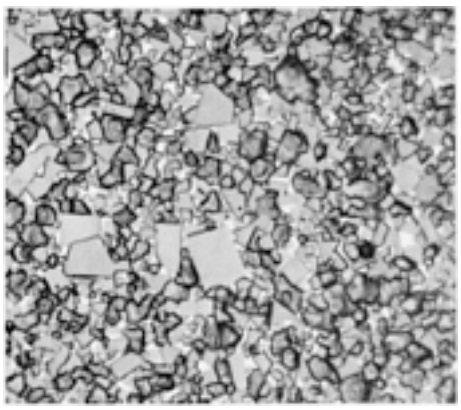

Fig. 25 78WC-15 (Ta,Ti,Nb,W)C-7Co alloy, 92.2 HRA. Angular, gray particles are tungsten carbide; heavily etched, rounded particles are mixed carbides. The cobalt binder is white. Murakami's reagent, 2 min. 1500×

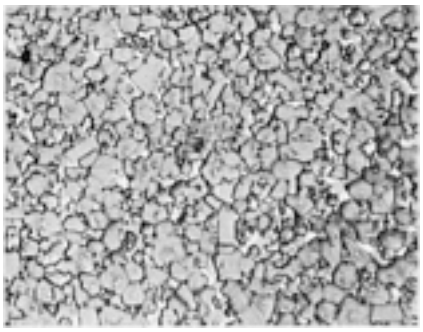

Fig. 26 73WC-21(Ta,Ti,Nb,W)C-6Co alloy, 92.9 HRA. This fine-grain microstructure consists of angular tungsten carbide, rounded mixed carbides, and white cobalt matrix. Murakami's reagent, 2 min. 1500×

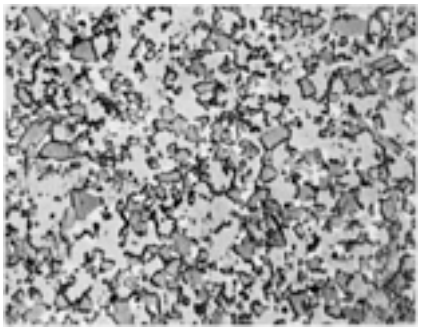

Fig. 27 43WC-50(Ta,Ti,Nb,W)C-6Co alloy, 90.0 HRA. Small, dark gray particles are tungsten carbide, larger, irregularly shaped, light gray areas are mixed carbides; white areas are the cobalt binder phase. Murakami's reagent, 2 min. 1500×

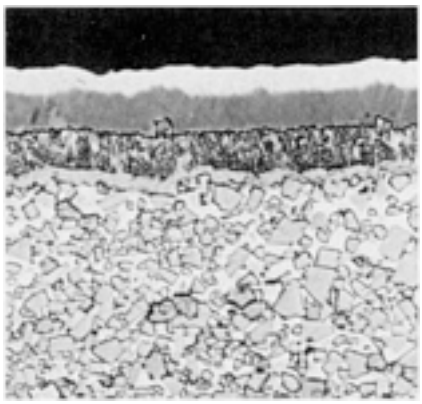

Fig. 28 86WC-8(Ta,Ti,Nb,W) C-6Co alloy, 91.6 HRA, with chemical vapor deposited coatings (from top) TiN, TiCN, and TiC. Angular, gray particles in the substrate are tungsten carbide; rounded particles are mixed carbides; and cobalt binder is white. Murakami's reagent, 2 min. 1500×

Fig. 29 Back-scattered scanning electron micrograph of 90WC-10Co alloy, 89.8 HRA. Gray particles

are tungsten carbide; cobalt binder phase is black. Compare this microstructure with that in Fig. 21. As-polished. 1500×

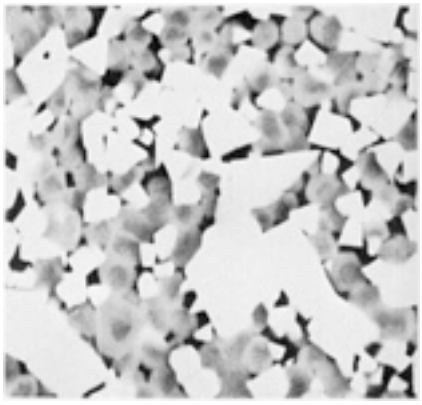

Fig. 30 Back-scattered scanning electron micrograph of 76WC-16(Ta,Ti,Nb,W)C-8Co alloy, 92.2 HRA. Light gray, angular particles are tungsten carbide, dark gray, rounded particles are mixed carbides; and cobalt binder is black. Compare this structure with Fig. 25. Murakami's reagent, 2 min. 1500×

Reference cited in this section

5. "Standard Method for Metallographic Determination of Microstructure in Cemented Carbides," B 657, *Annual Book of ASTM Standards*, Vol 02.05, ASTM, Philadelphia, 1984, p 538-542

Copyright © 2002 ASM International®. All Rights Reserved.

<Previous section in this article